Available online at www.sciencedirect.com
ScienceDirect
Nuclear Instruments and Methods in Physics Research A 589 (2008) 318–329
NUCLEAR INSTRUMENTS & METHODS IN PHYSICS RESEARCH Section A
www.elsevier.com/locate/nima

A Ramsey apparatus for the measurement of the incoherent neutron scattering length of the deuteron

F.M. Piegsa[a,b,*], B. van den Brandt[a], H. Glättli[c], P. Hautle[a], J. Kohlbrecher[a], J.A. Konter[a], B.S. Schlimme[d], O. Zimmer[b,e]

[a] Paul Scherrer Institute, CH-5232 Villigen PSI, Switzerland
[b] Physics Department, TU München, D-85748 Garching, Germany
[c] SPEC and LLB, CEA Saclay, F-91191 Gif-sur-Yvette Cedex, France
[d] Institut für Kernphysik, Johannes Gutenberg-Universität, D-55099 Mainz, Germany
[e] Institut Laue-Langevin, BP 156, 38042 Grenoble, France

Received 12 February 2008; accepted 16 February 2008
Available online 23 February 2008

Abstract

A Ramsey apparatus for cold, polarised neutrons is described, which enables us to measure neutron precession angles with an absolute accuracy of about 1°. This is necessary to perform a planned high-accuracy measurement of the incoherent neutron scattering length $b_{\mathrm{i,d}}$ of the deuteron. The performance of the apparatus is demonstrated in systematic stability measurements as well as in two selected examples using samples containing polarised nuclear spins.

PACS: 21.45.+v; 25.40.Dn; 28.20.Cz; 25.10.+s; 29.25.Pj; 76.70.Fz

Keywords: Few-body physics; Neutron physics; Spin-dependent scattering length; Ramsey resonance technique; Dynamic nuclear polarisation

1. Introduction

Originally introduced as a molecular beam resonance method, Ramsey's technique of separated oscillating fields has become a well-established tool in many areas of research. It is sensitive to spin-dependent interactions of particles with external fields, which are detected as a spin precession angle φ^*. For slow neutrons the method is employed in various ways. Most longstanding is the search for a non-vanishing electric dipole moment (EDM) of the neutron, which serves as a tool to investigate CP violation beyond the CKM mechanism. Another application is the measurement of the spin-dependent, *incoherent* neutron scattering length b_{i} of atomic nuclides. Here, the measured angle φ^* is due to the spin-dependent strong force between neutron and nucleus, and it is proportional to b_{i}. A convenient description parameterises the collective neutron optical effect of a nuclear polarised target as a neutron interaction with a *pseudomagnetic field*, introduced to underline the analogy with ordinary neutron Larmor precession in a magnetic field. The method was pioneered by a group from Saclay in the 1970s and provided values for more than 30 nuclides with applications in neutron scattering and for tests of nuclear models [1–5].

The present paper describes our development of an improved Ramsey setup, with the aim to perform an accurate measurement of the spin-dependent neutron scattering length $b_{\mathrm{i,d}}$ of the deuteron. This quantity represents an important input to new effective field theories of nuclear forces at low energy [6–8]. These theories are model-independent and able to provide, for the first time with an estimate of the theoretical uncertainty, reliable predictions of many important low-energy quantities, e.g. of processes in big-bang nucleosynthesis and stellar fusion. Observables are calculated as systematic expansions in terms of contact interactions, characterised by a few

*Corresponding author at: Paul Scherrer Institute, CH-5232 Villigen PSI, Switzerland. Tel.: +41 56 310 5395; fax: +41 56 310 3718.
E-mail address: florian.piegsa@psi.ch (F.M. Piegsa).

0168-9002/$ - see front matter © 2008 Elsevier B.V. All rights reserved.
doi:10.1016/j.nima.2008.02.020

so-called low-energy constants (LECs) that are determined by experiments. Best suited LECs to describe three-nucleon (3N) interactions, due to the absence of the Coulomb force, are the binding energy of the triton and the doublet neutron–deuteron (nd) scattering length $b_{2,\mathrm{d}}$. The reason of the high sensitivity of the latter to 3N forces is the absence of Pauli blocking in the doublet channel, since the incident neutron has its spin anti-parallel to the one bound in the deuteron. While the triton binding energy is known with an accuracy of 5×10^{-7}, the experimental knowledge of the nd doublet scattering length is only 6% [9]. This has motivated the present development to determine this crucial quantity with high-accuracy in an experiment proposed in Ref. [10]. The nd doublet scattering length can be obtained from a linear combination of the coherent and the incoherent ones, $b_{\mathrm{c,d}}$ and $b_{\mathrm{i,d}}$. The former one is already known very accurately and was recently even further improved in an interferometric measurement at NIST [11].

The first two sections of this article briefly recall the concept of the pseudomagnetic field and how Ramsey's technique is used to measure the pseudomagnetic precession angle. Next we describe in detail the components and the stabilisation of the Ramsey apparatus currently employed at the cold, polarised neutron beam FUNSPIN at the Paul Scherrer Institute. The performance of the apparatus is demonstrated with the results of two selected measurements in the final section. The apparatus described here is an improved version of the facility used previously in Saclay.

2. The pseudomagnetic field

The pseudomagnetic field is an intuitive way to describe the effect of a nuclear polarised target on the neutron spin. The s-wave scattering of a slow neutron by a nucleus is described by the bound scattering length b,

$$b = b_{\mathrm{c}} + \frac{2b_{\mathrm{i}}}{\sqrt{I(I+1)}}\vec{s}\cdot\vec{I} \tag{1}$$

consisting of a spin-independent part with the *coherent* scattering length b_{c}, and a spin-dependent component with the *incoherent* scattering length b_{i}, with $\vec{s}$ and $\vec{I}$ denoting the spins of the neutron and the nucleus [1]. Neutrons passing through a sample of polarised nuclei sense a spin-dependent Fermi potential $V_{\mathrm{F,spin}}$, which is proportional to b_{i} of the polarised nuclear species [12]. This potential due to the nuclear interaction can be expressed as

$$V_{\mathrm{F,spin}} = Nb_{\mathrm{i}}\frac{4\pi\hbar^2}{m_{\mathrm{n}}}\sqrt{\frac{I}{I+1}}\vec{P}\cdot\vec{s} = -\vec{B}^*\cdot\vec{\mu}_{\mathrm{n}}, \tag{2}$$

where m_{n}, γ_{n} and $\vec{\mu}_{\mathrm{n}}$ are the mass, the gyromagnetic ratio and the magnetic moment of the neutron. I is the spin of the nuclear species, present with number density N and polarisation vector $\vec{P}$. The proportionality $\vec{\mu}_{\mathrm{n}} = \gamma_{\mathrm{n}}\hbar\vec{s}$ is used to express the potential as an effective interaction between $\vec{\mu}_{\mathrm{n}}$ and a pseudomagnetic field $\vec{B}^*$. The interaction thus has the same form as that of $\vec{\mu}_{\mathrm{n}}$ with a real magnetic field and therefore leads to the same effects, such as the pseudomagnetic analogue of Larmor precession with an angular frequency $\omega^* = -\gamma_{\mathrm{n}}B^*$. Considering a polarised sample with a typical number density $N = 5\times10^{22}\,\mathrm{cm}^{-3}$ of hydrogen (deuterium) atoms [13,14], the corresponding pseudomagnetic fields are $B^*_{\mathrm{p}} \approx 3.1\cdot P_{\mathrm{p}}\,\mathrm{T}$ ($B^*_{\mathrm{d}} \approx 0.6\cdot P_{\mathrm{d}}\,\mathrm{T}$), where P_{p} (P_{d}) is the polarisation of the protons (deuterons).

The existence of a pseudomagnetic field was predicted by Barishevskii and Podgoretskii from an analysis of the neutron optical properties of a polarised target [15]. A resonance experiment by Abragam et al. [16] provided the first experimental demonstration using a sample of dynamically polarised protons in LMN.[1] Later pseudomagnetic precession detected with a Ramsey apparatus became a standard tool to determine incoherent scattering lengths (for an example of measurements of ^{1}H and ^{51}V see Ref. [17]).

In the general case of a sample consisting of various nuclear species k, the pseudomagnetic precession angle is given by

$$\varphi^*[\mathrm{rad}] = 2\lambda d\sum_k\sqrt{\frac{I_k}{I_k+1}}P_kN_kb_{\mathrm{i},k}, \tag{3}$$

where λ is the neutron de Broglie wavelength, and d is the thickness of the polarised sample. In principle, a sample containing a single polarised nuclear species is sufficient to determine the incoherent scattering length of this nucleus, if the neutron wavelength and the sample properties are known. In order to avoid the experimental difficulties associated with absolute measurements of number density and nuclear polarisation, which would limit considerably the final accuracy, we will adopt the method proposed in Ref. [10], which relies on a relative measurement employing a sample containing both protons and deuterons.

3. Ramsey's resonance method of separated oscillating fields

This section recalls the basic features of Ramsey's method [18] and provides formulas for the dependence of the observed signals from geometrical parameters, field strength and the width of the neutron wavelength distribution (instrumental parameters). A sketch of the Ramsey apparatus is shown in Fig. 1. A polarised neutron beam passes through a static magnetic field $\vec{B}_0$ in which two phase-locked $\pi/2$-resonance spin flippers are situated. Their fields $\vec{B}_1$ oscillate perpendicularly to $\vec{B}_0$ ($B_1 \ll B_0$), with an angular frequency ω close to the neutron Larmor frequency $\omega_0 = -\gamma_{\mathrm{n}}B_0$. The spin flippers have a length l and are separated by a distance L. The field amplitude B_1 is adjusted to result in a 90° rotation of the neutron spin in each spin flipper at resonance.

We first consider the ideal case of a fully polarised ($P_{\mathrm{n}} = 1$) and perfectly monochromatic beam with the

[1] Lanthanum magnesium nitrate, $La_2Mg_3(NO_3)_{12}\cdot 24H_2O$.

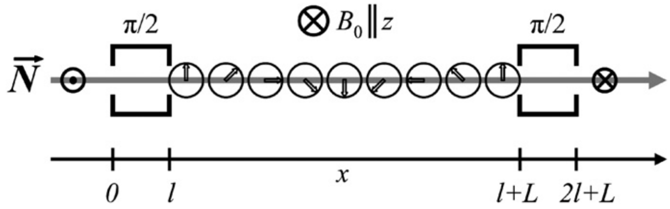

Fig. 1. Ramsey's resonance method of separated oscillating fields for cold neutrons at resonance condition. Polarised neutrons ($\vec{N}$) travel in x-direction through a constant magnetic field $\vec{B}_0$ pointing in z-direction. The neutron spins precess freely with their Larmor frequency $\omega_0 = -\gamma_n B_0$ across a distance L between two $\pi/2$-resonance spin flippers of the length l where their spin gets turned by 90° each.

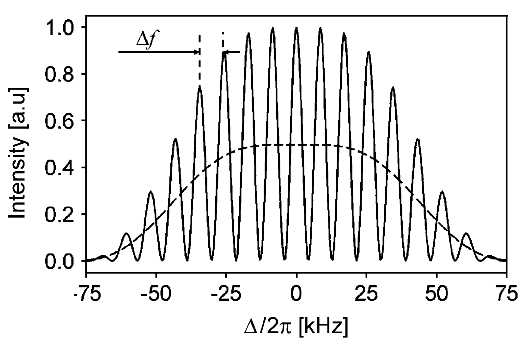

Fig. 2. Simulated Ramsey resonance signal. Probability to detect a 180°-flipped neutron (solid line) and the corresponding background resonance curve (dashed line). Used simulation parameters: $P_n = 1$, $\lambda_0 = 5\,\text{Å}$, $l = 10\,\text{mm}$, $L = 80\,\text{mm} \rightarrow \Delta f \approx 8.5\,\text{kHz}$, FWHM $\approx 88.6\,\text{kHz}$.

wavelength $\lambda_0 = h/m_n v_0$, where h is the Planck constant, v_0 is the neutron velocity, and m_n is the neutron mass. With the resonance condition $\Delta = \omega - \omega_0 = 0$ exactly fulfilled, the first spin flipper rotates the neutron spin into the plane perpendicular to $\vec{B}_0$. The subsequent Larmor precession stays in phase with the oscillating fields, and the second $\pi/2$-spin flipper thus completes the spin flip by 180°. For small deviations from $\Delta = 0$ the spin will still be rotated by about 90° in the first spin flipper, but subsequently run out of phase with the field in the second flipper. If, for example, an additional phase shift of 180° occurs, the neutron spin will be turned back in its initial direction.[2] The spin component antiparallel to the incoming polarisation as a function of Δ exhibits a characteristic wiggle pattern. It can be described by Eq. (A.11) derived in Appendix A, which gives the probability $\mathscr{W}(\Delta)$ for a 180° spin flip. This would be seen as an intensity oscillation after a polarisation analyser, as shown in Fig. 2. The theoretical difference Δf between two frequencies, where the probability for a 180° flip has a maximum, is given by

$$\Delta f \approx \frac{h}{m_n \lambda_0 L}\left(1 + \frac{4}{\pi}\frac{l}{L}\right)^{-1} \quad \text{for } L \gg l. \tag{4}$$

[2]This is easily understood, if one considers the spin flip process in the reference frame rotating with the angular frequency ω.

Further off resonance, one observes a damping of the amplitudes of the intensity oscillations due to the decreasing efficiency of the spin flippers. A formula for the "background resonance" part of the whole Ramsey signal is given in Eq. (A.14) and shown as a dashed line in Figs. 2 and 3. Its width depends on the time τ the neutron spends in the spin flippers and is found numerically,[3]

$$\text{FWHM [Hz]} \approx \frac{1.12}{\tau\,[\text{s}]} \approx \frac{4.43 \times 10^6}{\lambda_0\,[\text{Å}] \cdot l\,[\text{mm}]}. \tag{5}$$

So far we have not taken into account an additional precession angle φ^* of the neutron spin between the spin flippers, such as caused by the pseudomagnetic field of a nuclear polarised target. For a perfectly monochromatic beam it leads to a corresponding phase shift of the oscillatory part of the Ramsey signal, keeping the envelope of the wiggles unaffected.

Considering the case where the neutron beam has a wavelength distribution $p(\lambda)$, things become more complicated due to the velocity dependence of φ^*,

$$\varphi^*(\lambda) = \varphi_0^* \cdot \frac{\lambda}{\lambda_0}, \tag{6}$$

where φ_0^* is the precession angle of a neutron with wavelength λ_0. The resulting spread of φ^* around φ_0^* leads to a modification of the envelope of the Ramsey signal, whereas the phase shift of the wiggles within the envelope is still given by φ_0^* (for symmetric $p(\lambda)$). The corresponding probability $\mathscr{W}'$ for a 180° flip, given in Eq. (A.12), also takes a non-perfect neutron polarisation P_n into account. Examples of Ramsey signals for a wavelength distribution $\Delta\lambda/\lambda_0 = 0.06$ are shown in Fig. 3. As a result, the limited monochromacy of the beam imposes practical limits to the maximum phase shift, beyond which the wiggles become undetectable.

A perfectly homogeneous constant magnetic field $\vec{B}_0$ is not possible to provide. Indeed it is only necessary that the average field along the neutron flight path L between the spin flippers is equal to the field $B_{0,\text{rf}}$ at the sites of the spin flippers,

$$\langle B_0 \rangle = \frac{1}{L}\int_l^{l+L} |\vec{B}_0(x)|\,\mathrm{d}x = B_{0,\text{rf}} \tag{7}$$

because the validity of this equation already assures that the neutron spins precess on average in phase with the oscillatory fields of the spin flippers at $\Delta = 0$. This means that one has rather to cope with the stabilisation of the magnetic field than with providing a very high homogeneity.

4. The Ramsey apparatus

In this section we describe the actual setup of our Ramsey apparatus at the FUNSPIN beamline at the Paul Scherrer Institute [19].

[3]Calculated from Eq. (A.14) with $\mathscr{W} = \frac{1}{4}$.

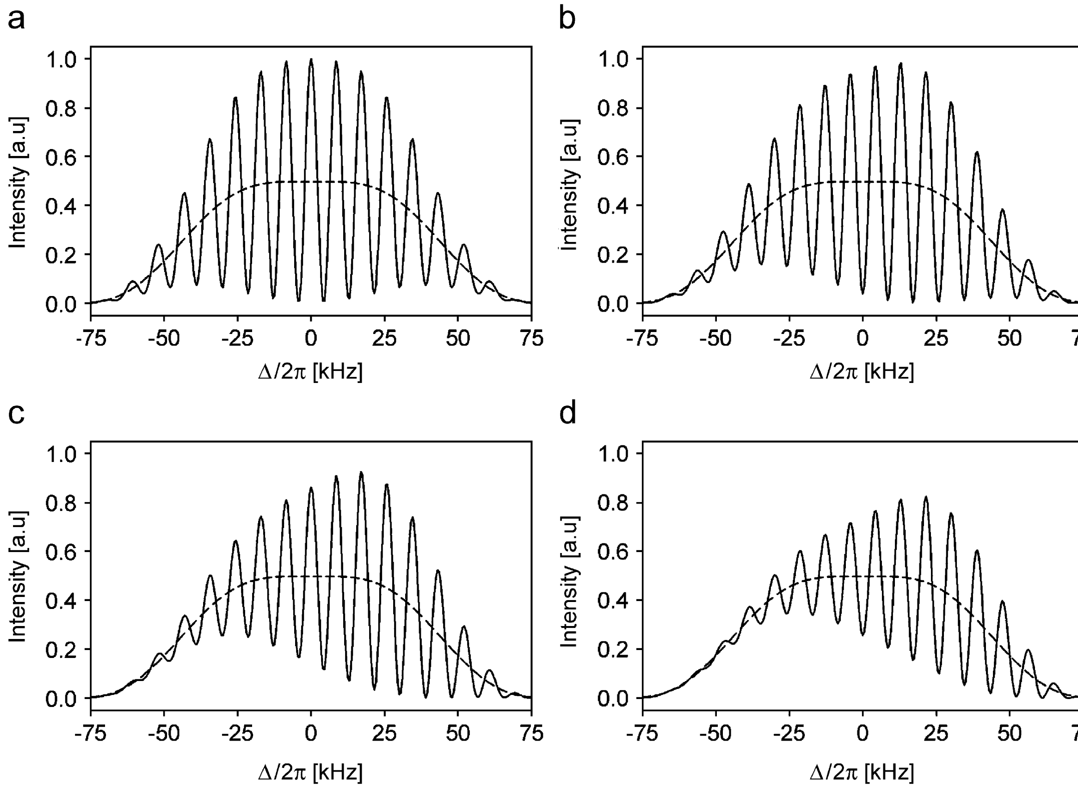

Fig. 3. Simulated Ramsey signals with an assumed Gaussian wavelength distribution with $\Delta\lambda/\lambda_0 = 0.06$ (respectively: $\sigma_\lambda/\lambda_0 = 0.026$). The damped oscillations move along the background resonance curve (dashed line) if the additional precession angle increases. (a) $\varphi_0^* = 0°$, (b) $\varphi_0^* = 900°$, (c) $\varphi_0^* = 1800°$ and (d) $\varphi_0^* = 2700°$. Further simulation parameters: $P_n = 1$, $\lambda_0 = 5\,\text{Å}$, $l = 10\,\text{mm}$, $L = 80\,\text{mm}$.

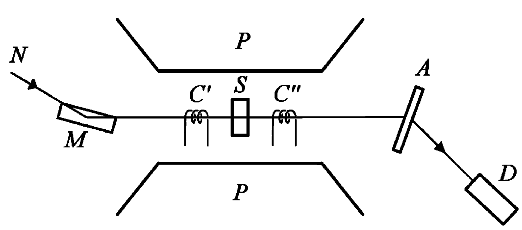

Fig. 4. Scheme of the principle setup of the Ramsey apparatus. The white polarised neutron beam (N) is monochromised by a NiTi-supermirror (M) and afterwards passes two $\pi/2$ radio frequency spin flipper coils (C′, C″) and the sample (S), which are placed between the pole pieces of a magnet (P). Finally the spin of the neutron is analysed in an analysing bender (A) and detected in a ^{3}He-gas tube detector (D).

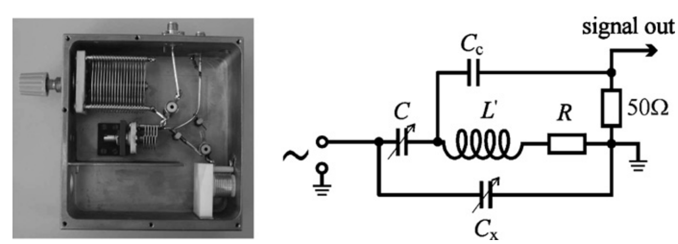

Fig. 5. Left: picture of an opened $\pi/2$-spin flipper (shielded brass case—size: $101.5 \times 109 \times 46\,\text{mm}^3$). The rf coil consisting of 0.8 mm thick silver wire is wound on a Macor® cylinder with a pitch of one turn per mm. Variable capacitors are used to tune the resonance circuit to about 73 MHz and to match it to 50 Ω. Right: scheme of the circuit. L' and R are the inductance and the ohmic resistance of the coil. $C = 1...5$ pF and $C_x = 20...300$ pF are the tunable capacitors and C_c serves as a coupling capacity to obtain a signal used for the feedback loop.

4.1. Overview

A scheme of the setup is shown in Fig. 4. The white polarised cold neutron beam (N) is first collimated by several diaphragms and afterwards deflected by about 3.2° on a neutron NiTi bandpass supermirror (M) [20]. This produces a Gaussian-shaped neutron wavelength spectrum with maximum at about 5 Å and a relative width $\Delta\lambda/\lambda_0$ of approximately 0.06 (FWHM). Along the beam path two radio frequency (rf) coils, (C′) and (C″), acting as $\pi/2$-spin flippers with length $l = 7\,\text{mm}$ and diameter 14 mm each, are placed in the 48 mm wide gap between the pole pieces (P) of an electromagnet, which provides the static field[4] $B_0 \approx 2.5\,\text{T}$. The sample (S) is placed between the $\pi/2$-spin flippers, which are separated by a distance[5] $L \approx 80\,\text{mm}$. They form the inductances of two matched resonant circuits for frequencies around 73 MHz, provided by a rf signal generator and two rf amplifiers (see Fig. 5). Their

[4] This large magnetic field is required by the dynamic nuclear polarisation method employed to polarise the sample (see Section 5.2).

[5] This distance corresponds roughly to the diameter of the pole shoes, which are specially shaped to help to fulfil the condition given in Eq. (7).

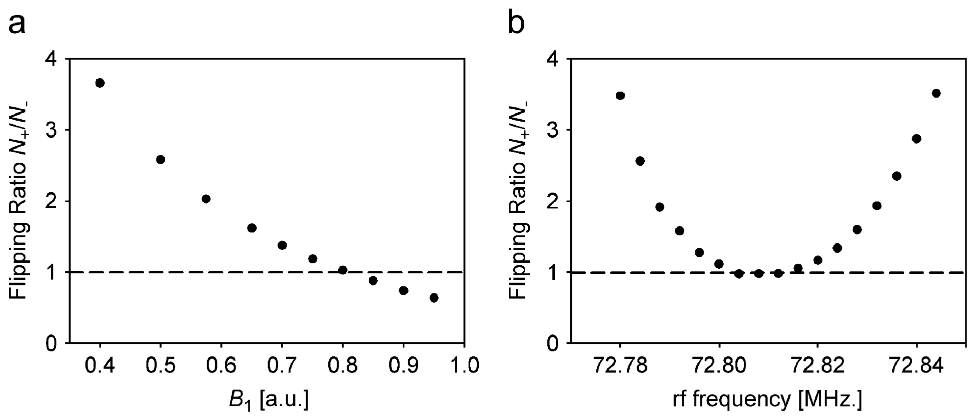

Fig. 6. Neutron flipping ratio measurements to adjust the rf field of one $\pi/2$-spin flip coil. (a) shows a scan of the oscillating field amplitude B_1 at a steady frequency of 72.815 MHz, (b) shows a scan of the rf frequency for a fixed field amplitude $B_1 = 0.8$ a.u.. The frequency where the flipping ratio has a minimum, here approximately 72.81 MHz, corresponds to the neutron Larmor frequency ω_0 in the steady magnetic field B_0 at the position of the rf coil.

linear oscillating fields $B_1'(t) = 2B_1' \cos(\omega t)$ and $B_1''(t) = 2B_1'' \cos(\omega t + \vartheta)$ are perpendicular to the static field and stabilised in phase and amplitude by a feedback loop. A field amplitude of about 10 G is required for a $\pi/2$-flip, for which the rf amplifiers have to deliver a power of about 5 W each. Therefore both rf coils have to be cooled with compressed air. Neutron polarisation analysis is performed with a supermirror bender (A), which has an analysing power of about 90% for 4 Å neutrons.[6] Finally, the neutrons are detected in a ^{3}He-gas detector (D). Count rates are normalised to the incident flux by a ^{235}U fission chamber with a dead time of 2.4 μs and an efficiency of 1.5×10^{-3}.

At the beginning of an experiment, the resonance frequencies of the spin flippers have to be tuned to the neutron Larmor frequency in the static field, $\omega_0 = -\gamma_n B_0$. Subsequently the amplitudes of the oscillating fields B_1' and B_1'' need to be adjusted separately such that each spin flipper turns the neutron spin by $\pi/2$. This is done by tuning the flipping ratio $FR = N_+/N_-$ to unity for one $\pi/2$-spin flipper, while the other $\pi/2$-spin flipper is turned off and vice versa (see Fig. 6). N_+ and N_- are the count rates for the adiabatic π-flipper of the beamline switched on and off.

Our desired accuracy of about 1° for the phase shift determination of the Ramsey signals requires high stability of the magnetic field and the spin flippers. The following sections describe how this is achieved.

4.2. Magnetic field stabilisation

The static magnetic field B_0 is monitored by means of the proton resonance signal of a commercial NMR probe operated at room temperature and placed in between the pole pieces of the magnet close to the sample position. The field of 2.5 T can be kept constant within ±0.8 μT using the monitored signal to regulate the current in the magnet.

[6]This has been measured at the neutron reflectometer Morpheus at SINQ at the Paul Scherrer Institute.

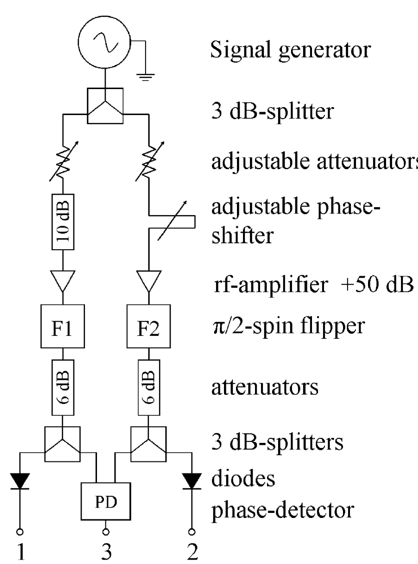

Fig. 7. Feedback loop of the two rf $\pi/2$-spin flippers (F1 and F2). The loop stabilises the relative phase ϑ as well as the individual amplitudes of both flippers. The three output lines (1, 2 and 3) are continuously sampled by a data aquisition system and are used as a feedback to control the adjustable phase-shifter and the adjustable attenuators.

As visible from the simulated data in Fig. 2 signal oscillations have a period of $\Delta f \approx 8.5$ kHz. The field stability stated before corresponds to an uncertainty of the neutron Larmor frequency of ±23 Hz. Hence the phase stability due to the magnetic field is about ±23 Hz/ 8.5 kHz × 360° ≈ ±1°.

4.3. Spin flipper feedback loop

The relative phase ϑ and the individual amplitudes B_1' and B_1'' of the two rf $\pi/2$-spin flippers are stabilised using a feedback loop, which is shown in Fig. 7. The rf signal of a signal generator is split into two branches by a 3 dB-splitter. The signal in each branch passes an attenuator adjustable by means of a DC voltage. The signal in branch one is then further attenuated to compensate the throughput loss of the controllable phase-shifter in branch two. Both signals then serve as inputs for two +50 dB rf power amplifiers feeding the matched resonant circuits of the spin flippers (see Fig. 5).

By capacitive coupling each spin flipper delivers a rf output signal. This allows us on one hand to determine the amplitudes of the oscillating magnetic fields using rf detector diodes. On the other hand the signals feed a phase-detector, which produces a DC voltage proportional to $\sin\vartheta$. The three DC voltages, from the two diodes and the phase-detector, are permanently sampled by a data aquisition system, which controls the input voltages of the adjustable phase-shifter and the adjustable attenuators by means of a PID algorithm.

With this feedback loop the DC voltages corresponding to the field amplitudes (output lines 1 and 2 in Fig. 7) can routinely be held stable within better than $\pm 0.2\%$ for each spin flipper, while the DC voltage corresponding to the relative phase (output line 3 in Fig. 7) can be held zero within ± 10 mV. By observing the phase of the Ramsey signal for systematically misadjusted settings for the amplitudes and the relative phase ϑ, one can link these DC voltage stabilities to the phase stability of the Ramsey signal (see Section 4.5). This leads to a conservatively estimated phase stability of the Ramsey signal, firstly of $\pm 0.1^\circ$ as a result of the stabilisation of ϑ, and secondly of $\pm 0.1^\circ$ for each spin flipper due to the stabilisation of the oscillating field amplitude. This yields an overall stability of the Ramsey signal due to the spin flippers of better than $\pm 0.3^\circ$.

4.4. Ramsey frequency scans

In Fig. 8a a typical Ramsey signal is shown, which was obtained with our setup by sweeping the frequency of the $\pi/2$-spin flippers in steps of 0.5 kHz from 72.75 to 72.87 MHz. Contrary to the simulated data shown before, the neutron spin analyser in our setup is transparent for the opposite spin component, which leads to an inversion of the Ramsey signal. Further comparison of the simulated and measured data reveals that the period of the Ramsey oscillations of $\Delta f \approx 8.74$ kHz is close to the expected value of about 8.5 kHz, whereas the width of about 70 kHz of the background resonance curve is much narrower than the FWHM of about 128 kHz expected according to Eq. (5) for rf coils with length $l = 7$ mm. This might be due to the fringe fields extending out of the coils along the beam path, resulting in an effective coil length l_{eff} of about 12.5 mm.

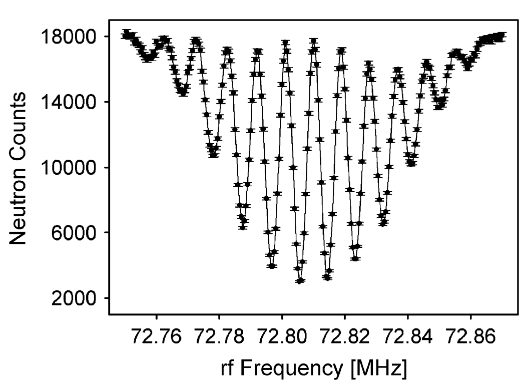

Fig. 8. Typical Ramsey resonance signal (frequency scan) measured with our setup without additional phase shift ($\varphi_0^* = 0^\circ$). The measuring time for each data point was approximately 12 s, which corresponds to about 10^5 neutron counts on the monitor detector.

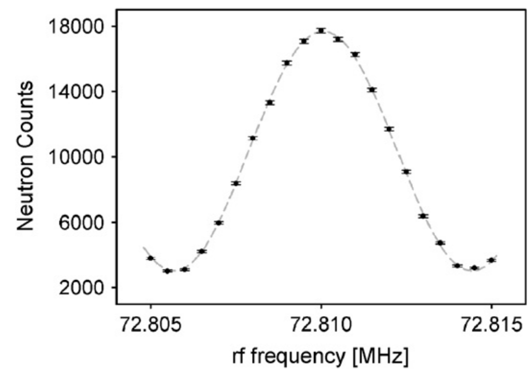

Fig. 9. Excerpt of the complete Ramsey signal shown in Fig. 8. The sinusoidal fit (dashed curve) on the 21 data points delivers a value of $\Delta f = (8.74 \pm 0.03)$ kHz for the period and of $\varphi = (-87.5 \pm 0.4)^\circ$ for the phase with respect to 72.81 MHz.

The quality of the measured Ramsey signals, with a signal-to-noise ratio of about 6 in the centre of the resonance, is very well suited to achieve a high precision in determining phase shifts. For that purpose it is more efficient to measure only the centre part of the resonance rather than to sweep over the whole resonance. This saves measuring time without loss in precision. A scan of 21 data points with a frequency step size of 0.5 kHz samples more than one oscillation of the Ramsey signal and can be fitted using a simple sinusoidal fit, like presented in Fig. 9. Instabilities have a minor influence on the accuracy of the phase extraction, because although the individual data point might scatter statistically with $\pm 1^\circ$, for a whole set of 21 data points this reduces by a factor $\sqrt{21}$, i.e. to a statistical uncertainty of only $\pm 0.2^\circ$.

4.5. Two-beam method and relative phase stability

The accuracy of the phase measurement can be strongly improved if one analyses simultaneously two separate beams passing through the Ramsey apparatus. By subtraction of the phases measured for each of the beams, a common phase drift can be efficiently removed, as it might for instance be caused by day–night temperature changes in the experimental hall. Practically, the incident beam is split into an upper and a lower beam, with adjustable diameters of typically 3 mm and a distance of the beam-centres of 6 mm, by means of Cd diaphragms placed before the first

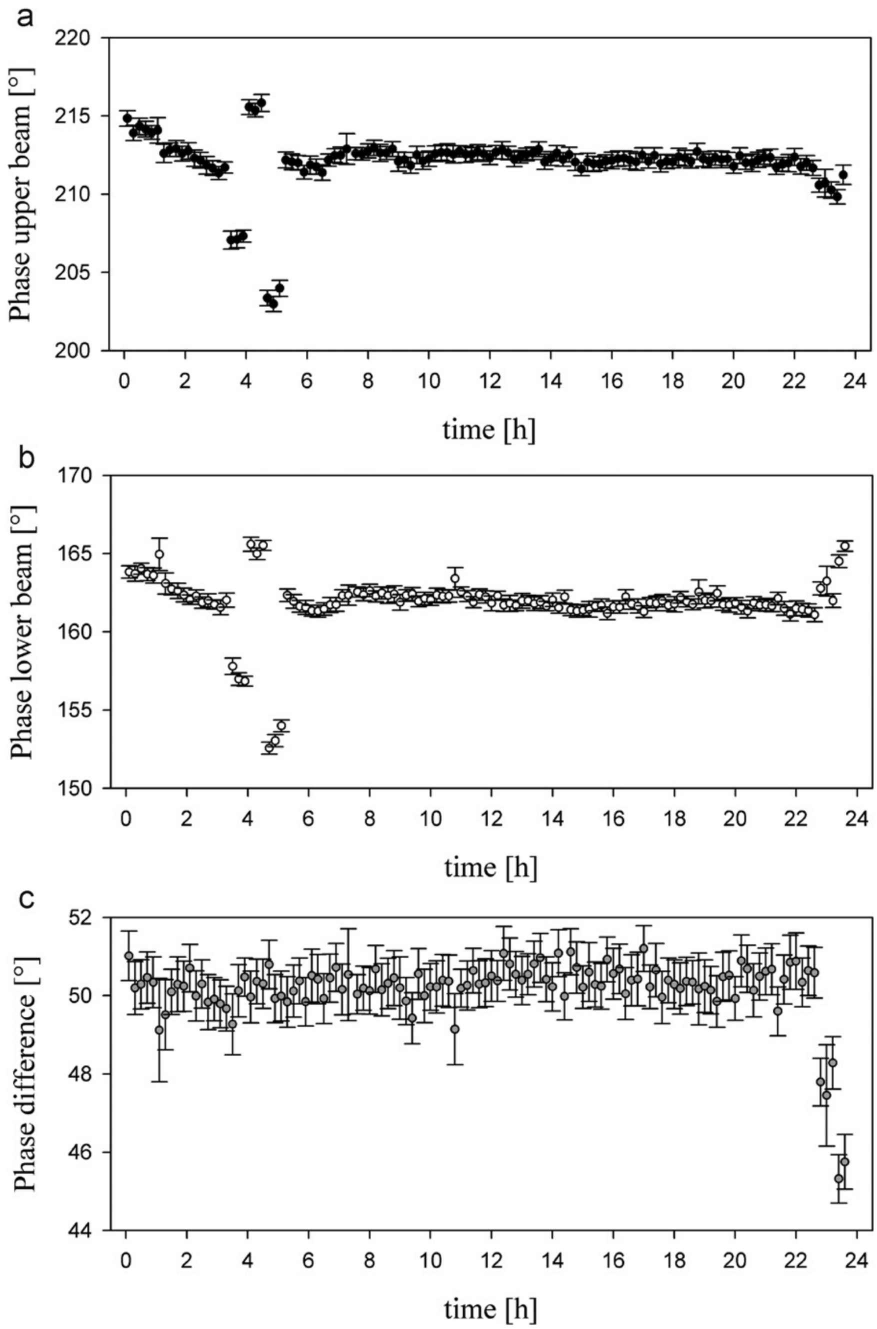

Fig. 10. Demonstration of the phase stability of the Ramsey setup. Plots (a) and (b) show the individual phases of the upper and the lower neutron beam measured continuously over almost 24 h. Plot (c) shows the phase difference of the two beams. The jumps in the individual beam phases and the phase difference from the third to the fifth hour and at the end of the measurement run are due to intentional misadjustments of the spin flippers. For the reason of visibility only every second measured point is plotted.

and after the second $\pi/2$-spin flipper. The upper beam passes through the sample, whereas the lower beam serves as a reference passing by the sample. They are detected behind the spin analysing bender by two ^{3}He-gas detectors.

To avoid mixing of the two neutron beams, the incident beam must already be well collimated before it gets split up by the Cd diaphragms. This is achieved by several ^{6}Li diaphragms placed in front of the monochromating supermirror. The mixing of the beams thus could be kept below 1%. Simulations show that in the worst case of a 90° phase difference between the two beams, this would lead to a phase shift of about 0.6° in the Ramsey signals of both partial beams, assuming they have the same intensity. The beam mixing was measured by comparing the background corrected count rate in the detector of one beam with and without covering its hole in the first beam splitting diaphragm.

Employing this two-beam method a long measurement was performed to test the stability. We repeatedly measured Ramsey signals during almost 24 h, like the one shown in Fig. 9. The individual phase of each beam and the phase difference was then determined. Fig. 10 shows that indeed the phases of the individual beams exhibit a common drift, leading to a constant phase difference, which scatters around the mean value by $\pm 0.36^\circ$, while the average length of the errorbars, occurring only from the sinusoidal fit, is 0.65°. The two jumps in the phase difference at the end of the whole run, each of about 2°, were caused by an intentional drastic increase of the oscillating field amplitude of the first spin flipper, first by 6% and then by 12%.

As expected, changes in the relative phase ϑ of the spin flippers lead to jumps in the individual beam phases, but have no influence on the phase difference. This was tested, while during the time from the third to the fifth hour the set value of the DC voltage for the relative phase of the spin flippers was intentionally misadjusted three times from 0 to +0.5 V, −0.5 and +1.0 V and finally back to 0 V (output line 3 in Fig. 7). More extensive studies showed that a change of this set value delivers equal-sized phase shifts in both beams by $(8.1 \pm 0.1)^\circ/\mathrm{V}$. Note that the measured stability of $\pm 10\,\mathrm{mV}$ given in Section 4.3 then corresponds to a stability of better than $\pm 0.1^\circ$.

The absence of an effect in the phase difference plot demonstrates the power of the two-beam method, which was already successfully employed in a measurement of the incoherent scattering length of ^{3}He [21].

5. Measurements with nuclear polarised samples

In this section two examples for the measurement of the pseudomagnetic precession angle φ^* due to polarised nuclei in solid polystyrene samples are presented. To reach a sizeable nuclear polarisation the samples have to be cooled to very low temperatures. This has been accomplished in the first case by employing a ^{4}He evaporation cryostat reaching temperatures down to 1 K and in the second case by a ^{3}He–^{4}He dilution refrigerator of the same type as described in Ref. [22] with a base temperature below 100 mK. In the latter case the sample was placed inside a target cell filled with liquid ^{4}He, thermally anchored to the mixing chamber of the cryostat, to avoid that the neutron beam has to pass through the strongly absorbing ^{3}He. Both cryostats were specially designed to firmly fit in between the pole pieces of our 2.5 T magnet and are equipped with a NMR system to observe the nuclear polarisation of the samples [23].

5.1. Proton spins in thermal equilibrium

The first sample was a $14 \times 14 \times 3\,\mathrm{mm}^3$ n-polystyrene slab with a weight of 606 mg. It was placed in the upper beam of the Ramsey apparatus such that the neutrons see a target thickness of $d = 3\,\mathrm{mm}$. The proton spins in the sample were polarised by the so-called *brute force method.* In the high temperature limit the achievable spin polarisation is proportional to B/T_s (Curie's law), where B is the

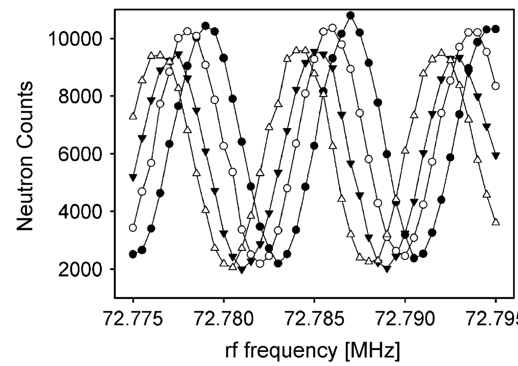

Fig. 11. Ramsey signals measured with a 3 mm thick n-polystyrene sample at four different temperatures: $T_s = 1.82$ K (white triangles), $T_s = 1.50$ K (filled triangles), $T_s = 1.27$ K (white circles) and $T_s = 1.09$ K (filled circles). With decreasing temperature the proton polarisation increases, which leads to a shift of the Ramsey oscillations to higher frequencies.

applied magnetic field and T_s is the temperature of the nuclear spin system.[7] In the case of proton spins the thermal equilibrium polarisation is given by

$$P_\mathrm{p} = \frac{\gamma_\mathrm{p} \hbar B}{2 k_\mathrm{B} T_\mathrm{s}} = 0.102\% \cdot \frac{B\,[\mathrm{T}]}{T_\mathrm{s}\,[\mathrm{K}]}, \tag{8}$$

where γ_p is the gyromagnetic ratio of the proton and k_B is Boltzmann's constant. Inserting Eq. (8) into Eq. (3) and using the proton number density of our sample of approximately 0.08 mol/ml and a neutron wavelength of 5 Å, leads to a pseudomagnetic phase shift due to the proton spins of

$$\varphi^* \approx 102^\circ \cdot \frac{d\,[\mathrm{mm}]}{T_\mathrm{s}\,[\mathrm{K}]}. \tag{9}$$

Fig. 11 shows several Ramsey signals taken at different temperatures of the sample. A temperature decrease causes an increase of the proton spin polarisation, which shifts the Ramsey oscillations to higher frequencies. The phase shifts of these oscillations could be determined with an accuracy of $\pm 0.9^\circ$. In Fig. 12 these are plotted against the inverse temperature $1/T_s$, showing the expected linear behaviour with a slope of $(115 \pm 3_\mathrm{stat} \pm 8_\mathrm{syst})^\circ\,\mathrm{K/mm}$, which is close to the estimated value given in Eq. (9). The systematical error is due to uncertainties of the neutron wavelength[8] and of the nuclear number density at 1 Kelvin and is estimated to be about 7% in total.

5.2. Dynamically polarised protons and deuterons

In the second example a deuterated plastic disc made out of d8-polystyrene was used as a sample [14]. The 25 mg disc had a diameter of 5 mm, a thickness of 1.2 mm and the degree of deuteration was about 97%. The deuterons and

[7]Note that for very low temperatures and high magnetic fields the nuclear relaxation time, i.e. the exponential time constant for the spin system to reach thermal equilibrium, can become very long.

[8]The neutron wavelength was not measured, but just calculated from the reflectivity curve of the supermirror.

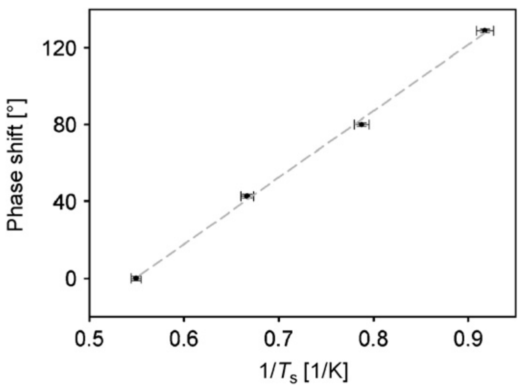

Fig. 12. Phase shift due to the decrease of the sample temperature and linear fit (dashed line). The phase shift of the data point measured at $T_s = 1.82$ K has been arbitrarily set to 0°. Errorbars: temperature ±1% and phase shift ±0.9°.

the residual protons were polarised by means of the *dynamic nuclear polarisation* method [1], which transfers the electron polarisation of admixed paramagnetic centres[9] to the nuclear spins. Proton (deuteron) polarisations of typically 40% (20%) were used and measured with a continuous wave Q-meter NMR system. Inserting these polarisation values and sample properties in Eq. (3) yields a pseudomagnetic phase shift of approximately $\varphi^* = \varphi^*_p + \varphi^*_d \approx 550° + 1650° = 2200°$ for 5 Å neutrons.

Fig. 13a shows the corresponding Ramsey signals for an unpolarised and dynamically polarised sample. The latter has a damped amplitude due to the large pseudomagnetic shift and possible polarisation inhomogeneities of the nuclei in the sample [24]. Due to asymmetric signal envelopes of the Ramsey oscillations at such large phase shifts (compare simulations in Fig. 3), it can be advantageous not to apply the standard sinusoidal fit as in the previous cases, but the following function:

$$a(\nu) = a_0 + a_1 \cdot \sin\left(\frac{2\pi}{\Delta f} \cdot \nu - \varphi\right) \cdot (1 + a_2 \cdot \nu + \mathcal{O}(\nu^2)), \quad (10)$$

where $a_2 \neq 0$ is the first order coefficient of an expansion describing the signal deformation. Careful comparisons between the two fit functions (sinusoidal and $a(\nu)$) show that the resulting value for the phase shift is equal within the errors of the fits, but that χ^2 is smaller for $a(\nu)$ (here: $\chi^2_{a(\nu)} < 2$).

Using Eq. (10) to fit the two signals in Fig. 13a delivers two slightly different periods of the Ramsey oscillations: $\Delta f_{\text{unpol}} = 8.82$ kHz and $\Delta f_{\text{pol}} = 8.89$ kHz. In order to determine the phase shift, one therefore has to define the period to a common fixed value Δf_{fixed} prior to the fit of both signals. Fig. 13b demonstrates that the relative phase shift of the sample beam $\Delta\varphi_{\text{sample}} = \varphi_{\text{sample,pol}} - \varphi_{\text{sample,unpol}}$ is almost unaffected by the choice of Δf_{fixed} and that the fit error becomes minimal around $\Delta f_{\text{fixed}} = 8.85$ kHz.

For the signals shown in Fig. 13a the relative phase shift is $\Delta\varphi_{\text{sample}} = (-29.2 \pm 0.6)°$ for the sample beam and $\Delta\varphi_{\text{ref}} = (+10.7 \pm 0.3)°$ for the reference beam, which passes by the sample. The total pseudomagnetic phase shift is given by

$$\Delta\varphi_{\text{total}} = n \times 360° + \Delta\varphi_{\text{sample}} - \Delta\varphi_{\text{ref}}, \quad (11)$$

where n can either be determined by successive destruction of the nuclear polarisation employing saturating rf-pulses or by nuclear polarisation decay (see Fig. 14). In this case $n = 6$, which leads to $\Delta\varphi_{\text{total}} = (2120.1 \pm 0.7)°$, where the relative accuracy of 4×10^{-4} is only due to the fit error.

Besides the fit, one has to take into account errors caused by the following sources:

- The phase stability of the Ramsey apparatus, which was shown to be ±0.36° in Section 4.5.
- The beam separation, leading in the worst case to be ±0.6° × 2, where the factor two takes into account that the beam mixing produces phase shifts in the sample and the reference beam.
- The nuclear polarisation relaxation during the measurement of the Ramsey signal, which leads to a signal drift of about 18°/h at $\varphi^* \approx 2000°$. This yields a systematical error of about ±1.5°, for a measurement time of 10 min per Ramsey signal consisting of 21 points. This error can be entirely attributed to the sample and is independent of the Ramsey apparatus.

Hence we get the total phase shift of $\Delta\varphi_{\text{total}} = (2120.1 \pm 0.7_{\text{fit}} \pm 0.4_{\text{stab}} \pm 1.2_{\text{beam}} \pm 1.5_{\text{sample}})°$, with four separate contributions of the error. The total relative accuracy of 2×10^{-3} is already about a factor 2 better than would be needed to reach the present precision of $b_{\text{i,d}}$.

Furthermore, it is possible to either correct for the systematic errors or to reduce them by improving the beam separation and by slowing down the nuclear polarisation relaxation, e.g. by decreasing the sample temperature.

6. Discussion and conclusions

The Ramsey apparatus described here is a powerful tool to determine precession angles of the neutron spin, e.g. due to pseudomagnetic fields. The use of the two-beam method enables us to measure phase shifts independently from global drifts. The reachable absolute accuracy due to the fit and the stability is about 1° within about 10 min of measuring time. The maximal observable phase shift is limited by the monochromacy of the neutron beam, which causes damping of the signal amplitude. With $\Delta\lambda/\lambda_0 = 0.06$ it is definitely possible to measure phase shifts of up to 2500°, which yields a relative accuracy of about 4×10^{-4}. This accuracy would allow for an improvement in precision of $b_{\text{i,d}}$ and the linearly dependent $b_{2,\text{d}}$ by up to a factor of 8.

[9] In this case the polystyrene was doped with deuterated nitroxyl radicals (d-TEMPO).

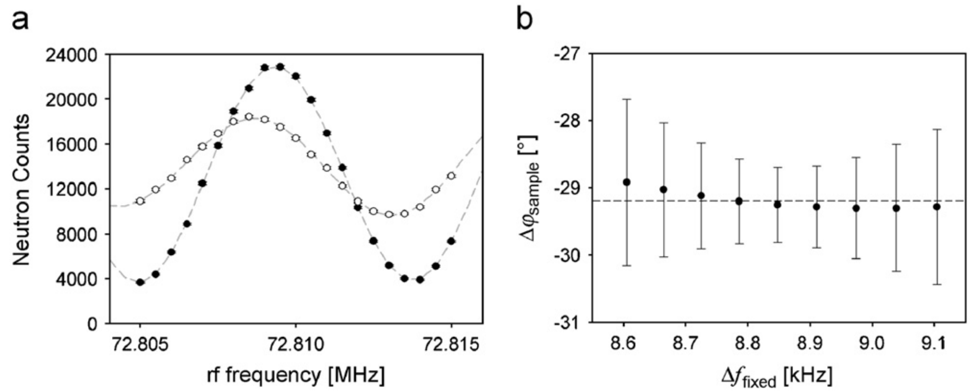

Fig. 13. (a) Ramsey signals for an unpolarised sample (filled circles) and a polarised sample leading to a phase shifted and damped signal (white circles) with the corresponding fits using Eq. (10) (dashed lines). (b) Dependence of the relative phase shift in the sample beam for different fixed values of the Ramsey oscillation period Δf_{fixed}. The dashed horizontal line marks a relative phase shift of $-29.2°$.

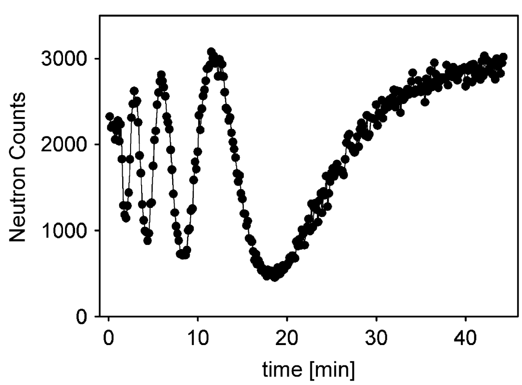

Fig. 14. Example of a determination of n by measuring the neutron counts at a fixed frequency of the Ramsey signal during the decay of the nuclear polarisation at 2.5 T and 1.1 K. Here the exponential decay time of the polarisation was approximately (5.4 ± 0.2) min and was measured using NMR. The total phase shift at $t = 0$ was approximately 1350°.

The following modifications of the Ramsey apparatus might lead to a further increase of the accuracy:

- A reduction of $\Delta\lambda/\lambda_0$ is advantageous to be able to measure even larger phase shifts than stated above. Of course this will be accompanied by longer measurement times due to the lower neutron flux.
- An increase (decrease) of the neutron wavelength λ_0 results in a setup, which is more (less) sensitive to spin-dependent potentials (see Eq. (3)).
- The use of spin flippers with transverse flat-coils, instead of the longitudinal solenoid coils, could provide more localised and homogeneous rf fields. This would allow for larger neutron beam cross-sections (higher flux) and would also reduce l_{eff}, which yields a wider "background resonance" of the Ramsey signal.
- An improvement of the phase stability of the Ramsey apparatus would be very challenging, since the present absolute stability of the magnetic field is already kept constant within $\pm 0.8\,\mu$T. An option would only be a decrease of the distance between the rf coils[10] L, which yields an increase of Δf (see Section 4.2).
- The magnetic field value of $B_0 = 2.5$ T of our apparatus is required by the dynamic nuclear polarisation mechanism employed to polarise the sample. However B_0 can also be chosen differently to best meet the appropriate conditions for other possible experiments, e.g. measurements of the neutron spin precession due to other polarised nuclei or other non-pseudomagnetic effects.

Thus it appears that the parameters of a Ramsey apparatus need to be changed according to the requirements of the performed measurement. The setup described here might also be useful for the determination of other spin-dependent scattering lengths or other possible purposes, as presented in Ref. [25].

Acknowledgements

This work was performed at the FUNSPIN beamline of the Swiss Spallation Neutron Source SINQ at the Paul Scherrer Institute in Switzerland. We especially acknowledge the technical support by W. Arrigoni, M. Schmutz and P. Schurter, whose outstanding skills have made this experiment possible. This work has been supported by the German BMBF under contract number 06MT252I.

Appendix A. Simulation of the Ramsey apparatus using time-evolution operators

The derivation given here differs slightly from that of Ramsey in Ref. [26] and employs the method of the time-evolution operators.[11] Instead of solving the Schrödinger equation to calculate the development of a state $|\psi(t)\rangle$ under the action of a Hamiltonian, which consists of a

[10]This is not possible with our apparatus, due to the special design of the pole shoes and the size of the cryostat situated between the spin flippers.

[11]An alternative derivation of this can be found in Ref. [27].

stationary and a time-dependent part

$$\hat{H}(t) = \hat{H}_0 + \hat{V}(t) \tag{A.1}$$

one can derive the time-evolution operator of the system [28], using the equation of motion

$$\mathrm{i}\hbar\frac{\partial}{\partial t}\hat{U}(t,t_0) = \hat{H}(t)\hat{U}(t,t_0), \tag{A.2}$$

where $|\psi(t)\rangle = \hat{U}(t,t_0)|\psi(t_0)\rangle$ and $|\psi(t_0)\rangle$ is an arbitrary initial state. The general solution of Eq. (A.2) is given by

$$\hat{U}(t,t_0) = \exp\left(-\frac{\mathrm{i}}{\hbar}\int_{t_0}^{t}\hat{H}(t')\,\mathrm{d}t'\right). \tag{A.3}$$

In our case we have a magnetic interaction of the magnetic moment of a spin $\frac{1}{2}$ particle, the neutron, with a magnetic field $\vec{B} = (B_x, B_y, B_z)$, which can be written as

$$\hat{H}(t) = -\frac{\hbar}{2}\gamma_\mathrm{n}\vec{\sigma}\cdot\vec{B} = -\frac{\hbar}{2}\gamma_\mathrm{n}\begin{pmatrix} B_z & B_x - \mathrm{i}B_y \\ B_x + \mathrm{i}B_y & -B_z \end{pmatrix}, \tag{A.4}$$

where $\vec{\sigma}$ is the vector of the Pauli matrices and γ_n is the gyromagnetic ratio of the neutron. The Ramsey apparatus can be divided in three regions (see Fig. 1). In the first (I) and the third (III) region a circular oscillating field with the amplitude B_1 flips the neutron spin by $\pi/2$ into and out of the plane perpendicular to the steady magnetic field $\vec{B}_0 = (0,0,B_0)$. In the second (II) region the neutron spin precesses freely in this plane with the Larmor frequency ω_0 and inside the sample with the shifted angular frequency $\omega_0 + \Delta\omega^*$ respectively. The time each of the rf fields acts on the neutron spin shall be denoted as τ and the time the neutron spends between the flippers as T. φ^* is the wavelength dependent pseudomagnetic precession angle due to the polarised nuclei in the sample as defined in Eq. (3).

To simplify the problem we consider our system in the reference frame rotating with the angular frequency ω, which is the frequency of the two rf fields [29]. One finds then for these three regions the following effective fields:

$$\vec{B}_{\mathrm{I,eff}} = \frac{1}{\gamma_\mathrm{n}}(-\omega_1, 0, \varDelta) \tag{A.5}$$

$$\vec{B}_{\mathrm{II,eff}} = \frac{1}{\gamma_\mathrm{n}}(0, 0, \varDelta) \tag{A.6}$$

$$\vec{B}_{\mathrm{III,eff}} = \frac{1}{\gamma_\mathrm{n}}(-\omega_1\cos\vartheta, -\omega_1\sin\vartheta, \varDelta), \tag{A.7}$$

where $\varDelta = \omega - \omega_0$ and $\omega_1 = -\gamma_\mathrm{n}B_1$ and ϑ is a fixed phase angle between the two circular oscillating fields. These effective magnetic fields have to be inserted now in Eqs. (A.3) and (A.4). If one takes also the additional precession angle φ^* into account one finds for the time-evolution operators setting $t_0 = 0$

$$\hat{U}_\mathrm{I}(\tau,0) = \begin{pmatrix} \cos\frac{\Omega\tau}{2} + \mathrm{i}\frac{\varDelta}{\Omega}\sin\frac{\Omega\tau}{2} & -\mathrm{i}\frac{\omega_1}{\Omega}\sin\frac{\Omega\tau}{2} \\ -\mathrm{i}\frac{\omega_1}{\Omega}\sin\frac{\Omega\tau}{2} & \cos\frac{\Omega\tau}{2} - \mathrm{i}\frac{\varDelta}{\Omega}\sin\frac{\Omega\tau}{2} \end{pmatrix} \tag{A.8}$$

$$\hat{U}_\mathrm{II}(T,0) = \begin{pmatrix} \mathrm{e}^{+(\mathrm{i}/2)(T\varDelta+\varphi^*)} & 0 \\ 0 & \mathrm{e}^{-(\mathrm{i}/2)(T\varDelta+\varphi^*)} \end{pmatrix} \tag{A.9}$$

$$\hat{U}_\mathrm{III}(\tau,0) = \begin{pmatrix} \cos\frac{\Omega\tau}{2} + \mathrm{i}\frac{\varDelta}{\Omega}\sin\frac{\Omega\tau}{2} & -\mathrm{i}\frac{\omega_1}{\Omega}\mathrm{e}^{-\mathrm{i}\vartheta}\sin\frac{\Omega\tau}{2} \\ -\mathrm{i}\frac{\omega_1}{\Omega}\mathrm{e}^{\mathrm{i}\vartheta}\sin\frac{\Omega\tau}{2} & \cos\frac{\Omega\tau}{2} - \mathrm{i}\frac{\varDelta}{\Omega}\sin\frac{\Omega\tau}{2} \end{pmatrix} \tag{A.10}$$

with $\Omega = \sqrt{\varDelta^2 + \omega_1^2}$. Without loss of generality we set $\vartheta = 0°$, so that $\hat{U}_\mathrm{I}(\tau,0) = \hat{U}_\mathrm{III}(\tau,0)$. The probability $\mathscr{W}$ for a transition from a spin state $|\uparrow\rangle = \binom{1}{0}$ to $|\downarrow\rangle = \binom{0}{1}$ is given by

$$\begin{aligned}\mathscr{W} &= |\langle\downarrow|\hat{U}_\mathrm{III}\cdot\hat{U}_\mathrm{II}\cdot\hat{U}_\mathrm{I}|\uparrow\rangle|^2 = |\langle\downarrow|\hat{U}_\mathrm{total}|\uparrow\rangle|^2 \\ &= \frac{4\omega_1^2}{\Omega^2}\sin^2\frac{\Omega\tau}{2}\left[\frac{\varDelta}{\Omega}\sin\frac{\Omega\tau}{2}\sin\frac{T\varDelta+\varphi^*}{2} - \cos\frac{\Omega\tau}{2}\right. \\ &\quad\left.\times\cos\frac{T\varDelta+\varphi^*}{2}\right]^2. \end{aligned} \tag{A.11}$$

The condition for the spin flippers to induce $\pi/2$ flips is $\omega_1 = \pi/(2\tau)$. Eq. (A.11) is identical to Eq. (12) in Ref. [26] and applies to only a single neutron velocity and a fully polarised neutron beam. Since the times τ and T are proportional to the neutron wavelength one has to perform an average over the wavelength distribution[12] $p(\lambda)$ of the neutrons and one also has to take the imperfection of the neutron polarisation P_n into account. Then one finds the probability $\mathscr{W}'$ to detect the spin state $|\downarrow\rangle$ behind the Ramsey apparatus as

$$\begin{aligned}\mathscr{W}' = \int_0^\infty p(\lambda)\left[\frac{1+P_\mathrm{n}}{2}|\langle\downarrow|\hat{U}_\mathrm{total}|\uparrow\rangle|^2\right. \\ \left.+\frac{1-P_\mathrm{n}}{2}|\langle\downarrow|\hat{U}_\mathrm{total}|\downarrow\rangle|^2\right]\mathrm{d}\lambda. \end{aligned} \tag{A.12}$$

Additionally two approximations can be applied on Eq. (A.11). The first one considers only frequencies very close to the resonance, so that $\omega_1 \gg \varDelta$:

$$\mathscr{W} \to \left[\frac{\varDelta}{\omega_1}\sin\frac{T\varDelta+\varphi^*}{2} - \cos\frac{T\varDelta+\varphi^*}{2}\right]^2. \tag{A.13}$$

From this, one can estimate the frequency distance Δf between two oscillation maxima, using only the first order

[12] Normalised wavelength distribution: $\int_0^\infty p(\lambda)\,\mathrm{d}\lambda = 1$.

term of the Taylor expansion of the tan-function around $\pi/2$. The result is given in Eq. (4) in Section 3. The other important approximation delivers the shape of the background resonance curve of the Ramsey signal (see Fig. 2), on substituting the fast oscillating terms $\sin T\Delta + \varphi^*/2$ and $\sin^2 T\Delta + \varphi^*/2$ by their average values 0 and $\frac{1}{2}$

$$\mathscr{W} \rightarrow \frac{2\omega_1^2}{\Omega^2} \sin^2 \frac{\Omega\tau}{2} \left[\left(\frac{\Delta}{\Omega}\right)^2 \sin^2 \frac{\Omega\tau}{2} + \cos^2 \frac{\Omega\tau}{2} \right]. \tag{A.14}$$

References

[1] A. Abragam, M. Goldman, Nuclear Magnetism: Order and Disorder, Oxford University Press, Oxford, 1982.
[2] H. Glättli, G.L. Bacchella, M. Fourmond, A. Malinovski, P. Mériel, M. Pinot, P. Roubeau, A. Abragam, J. Phys. 40 (1979) 629.
[3] P. Roubeau, A. Abragam, G.L. Bacchella, H. Glättli, A. Malinovski, P. Meriel, J. Piesvaux, M. Pinot, Phys. Rev. Lett. 33 (1974) 102.
[4] A. Malinovski, J. Coustham, H. Glättli, Nucl. Phys. A 365 (1981) 103.
[5] A. Abragam, G.L. Bacchella, H. Glättli, P. Meriel, J. Piesvaux, M. Pinot, J. Phys. Lett. 36 (1975) L-263.
[6] E. Epelbaum, A. Nogga, W. Glöckle, H. Kamada, U.-G. Meißner, H. Witala, Phys. Rev. C 66 (2002) 064001.
[7] J.-W. Chen, G. Rupak, M.J. Savage, Nucl. Phys. A 653 (1999) 386.
[8] P.F. Bedaque, H.-W. Hammer, G. Rupak, H. Grießhammer, Nucl. Phys. A 714 (2003) 589.
[9] W. Dilg, L. Koester, W. Nistler, Phys. Lett. B 36 (1971) 208.
[10] B. van den Brandt, H. Glättli, H. Gießhammer, P. Hautle, J. Kohlbrecher, J.A. Konter, O. Zimmer, Nucl. Instr. and Meth. A 526 (2004) 91.
[11] K. Schoen, D.L. Jacobson, M. Arif, P.R. Huffman, T.C. Black, W.M. Snow, S.K. Lamoreaux, H. Kaiser, S.A. Werner, Phys. Rev. C 67 (2003) 044005.
[12] E. Fermi, Ric. Sci. 7 (1936) 13.
[13] B. van den Brandt, E.I. Bunyatova, P. Hautle, J.A. Konter, S. Mango, Nucl. Instr. and Meth. A 446 (2000) 592–599.
[14] B. van den Brandt, E.I. Bunyatova, P. Hautle, J.A. Konter, Nucl. Instr. and Meth. A 526 (2004) 53.
[15] V.G. Baryshevskii, M.I. Podgoretskii, J. Exp. Theor. Phys. 20 (1965) 704.
[16] A. Abragam, Trends in Physics, European Physical Society, Geneva, Switzerland, 1973, p. 177.
[17] A. Abragam, G.L. Bacchella, H. Glätti, P. Meriel, M. Pinot, J. Piesvaux, Phys. Rev. Lett. 31 (1973) 776.
[18] N. Ramsey, Molecular Beams, Oxford University Press, Oxford, 1956.
[19] J. Zejma, G. Ban, M. Beck, A. Bialek, K. Bodek, G. Frei, Ch. Hilbes, G. Kühne, P. Gorel, K. Kirch, et al., Nucl. Instr. and Meth. A 539 (2005) 622.
[20] M. Ay, C. Schanzer, M. Wolff, J. Stahn, Nucl. Instr. and Meth. A 562 (2006) 389.
[21] O. Zimmer, G. Ehlers, B. Farago, H. Humblot, W. Ketter, R. Scherm, EPJ direct A 1 (2002) 1.
[22] B. van den Brandt, J.A. Konter, S. Mango, Nucl. Instr. and Meth. A 289 (1990) 526.
[23] B. van den Brandt, H. Glättli, H. Grießhammer, P. Hautle, J. Kohlbrecher, J.A. Konter, F.M. Piegsa, J.P. Urrego-Blanco, O. Zimmer, Proceedings of the 17th International Spin Physics Symposium SPIN 2006, Kyoto, Japan, 2–7 October 2006, AIP Conf. Proc. 915 (2007) 769.
[24] B. van den Brandt, H. Glättli, H. Grießhammer, P. Hautle, J. Kohlbrecher, J.A. Konter, F.M. Piegsa, B.S. Schlimme, J.P. Urrego-Blanco, O. Zimmer, Proceedings of the 14th International Conference on Particles and Nuclei PANIC 2005, Santa Fe, New Mexico, USA, 24-28 October 2005, AIP Conf. Proc. 842 (2006) 814.
[25] F.M. Piegsa, B. van den Brandt, P. Hautle, J.A. Konter, Nucl. Instr. and Meth. A 586 (2008) 15.
[26] N. Ramsey, Phys. Rev. 78 (1950) 695.
[27] R. Golub, R. Gähler, T. Keller, Am. J. Phys. 62 (1994) 779.
[28] J.J. Sakurai, Modern Quantum Mechanics, second ed., Addison-Wesley, Reading, MA, 1995.
[29] C.P. Slichter, Principles of Magnetic Resonance, third ed., Springer, Berlin, 1996.